JOURNAL OF GEOPHYSICAL RESEARCH, VOL. 102, NO. D12, PAGES 13,527–13,534, JUNE 27, 1997

A modeling study of the effect of drizzle on cloud optical depth and susceptibility

Graham Feingold

Cooperative Institute for Research in the Atmosphere and NOAA Environmental Technology Laboratory
Boulder, Colorado

Reinout Boers

Division of Atmospheric Research, CSIRO, Aspendale, Victoria, Australia

Bjorn Stevens and William R. Cotton

Department of Atmospheric Science, Colorado State University, Fort Collins

Abstract. This paper examines the impact of drop spectral broadening, generated by the collection process, on the optical depth, cloud albedo, and susceptibility of marine stratocumulus clouds. The results are arrived at using (1) the output from a simple box model calculation of collection and (2) the output from an eddy-resolving model of stratocumulus clouds that explicitly represents the size distribution of the drops. It is shown that commonly used relationships for cloud optical properties developed for narrow spectra do not generally apply to spectra undergoing spectral broadening. The optical depth dependence on the drop number concentration to the one-third power is shown to be an overestimate of the optical depth when spectra broaden through collection. In addition, the cloud susceptibility dependence on drop number is shown to be larger for spectra experiencing broadening than for narrow spectra.

1. Introduction

The radiative forcing of the Earth-atmosphere system by clouds is well recognized as a central component of the climate system [e.g., *Twomey*, 1974, 1977]. Although macroscale properties such as cloud cover, depth, and spatial inhomogeneity are of obvious importance in evaluating forcing, knowledge of cloud microphysical properties is also important [e.g., *Stephens*, 1978]. It is well known that the cloud condensation nucleus (CCN) concentration controls cloud droplet number concentration N; for a given cloud liquid water content (LWC), N determines the droplet effective radius r_e, the ratio between the integrated droplet volume to the integrated surface area. Radiative parameters such as single scattering albedo, and the asymmetry parameter g are dependent on r_e, and cloud optical depth τ is inversely proportional to r_e [e.g., *Stephens*, 1978; *Slingo*, 1989], so that characterization of either N or r_e together with LWC is critical if cloud forcing is to be evaluated.

Boundary layer clouds such as marine stratocumulus represent a class of clouds with a potentially significant impact on climate. By modifying the Earth's albedo compared with the underlying ocean, they have a strong impact on shortwave radiation, but being low level clouds, they radiate in the longwave at approximately the same temperature as the surface, so that there is no compensating effect for the shortwave forcing. Moreover, they occur with high frequency and have extensive spatial coverage (annually averaged cloud cover of 34% [*Warren et al.*, 1986]). For this reason, much effort has been invested in studying this class of cloud through intensive field campaigns (First ISCCP Regional Experiment (FIRE)–Stratocumulus [*Albrecht et al.*, 1988], Atlantic Stratocumulus Transition Experiment (ASTEX) [*Albrecht et al.*, 1995], Southern Ocean Cloud Experiment (SOCEX) [*Boers et al.*, 1996]) and through modeling studies [e.g., *Moeng*, 1986; *Albrecht*, 1993; *Kogan et al.*, 1995; *Stevens et al.*, 1996].

Numerous studies have investigated the relationship between CCN concentration and drop concentration N [e.g., *Twomey*, 1959; *Leaitch et al.*, 1992], as well as the relationships between cloud optical depth τ and N and between cloud albedo A and N [e.g., *Platnick and Twomey*, 1994]. In general, these relationships have been developed for nonprecipitating clouds with narrow, unimodal spectra. When drops larger than about 20 μm (radius) are formed via a number of possible (although uncertain) mechanisms, drizzle-sized drops can be formed through collection (collision-coalescence). In this case, droplets from the narrow spectra are removed to form drizzle-sized drops. The resulting spectra are broader and may or may not exhibit bimodality, depending on the degree of collection. The size of the drizzle drops is of the order of 100 μm depending on the depth of the cloud and the size of the largest (nondrizzle) droplets [*Nicholls*, 1984; *Frisch et al.*, 1995]. Thus the collection process affects the drop spectrum by simultaneously reducing the drop concentration and creating a broader spectrum; in so doing, it impacts the various parameters that are derived from the drop spectrum, as will be shown in section 2.

There is mounting evidence from observational studies [*Austin et al.*, 1995; *Bretherton et al.*, 1995; *Boers et al.*, 1996] attesting to the prevalence of collection and drizzle formation in stratocumulus clouds at diverse geographical locations. *Boers et al.* [1996] estimated from their observations that the formation of drizzle and its associated reduction in droplet number

Paper number 97JD00963.
0148-0227/97/97JD-00963$09.00

concentration was responsible for a reduction of up to 18% in cloud top albedo. The goal of this paper therefore is to revisit some of the relationships between radiatively important parameters and to examine their applicability to droplet spectra undergoing spectral broadening. In particular, the optical depth and susceptibility dependences on N are of interest. A framework of constant LWC has been chosen [e.g., *Platnick and Twomey*, 1994] because the collection process conserves LWC. The impact of a variable LWC, although of interest, is not addressed here. A theoretical/numerical modeling approach has been adopted, as very few observations are available to shed light on the collection process. It is hoped that this study will elucidate the impact of this process and guide our attempts to find observational support for the ideas expressed herein.

The study consists of two parts. In the first part a box model simulating stochastic collection is used to examine the influence of collection on typical droplet spectra, and its influence on τ and susceptibility S (at constant LWC) is computed. An analysis of the relationships between τ and N and between S and N, for situations where the drop spectrum is changing as a result of the collection process rather than of varying CCN concentrations, is presented. To capture the complexity of real clouds, the second part of this paper includes simulations of stratocumulus clouds using an eddy-resolving model coupled to a microphysical model that explicitly represents the drop size spectra. A case study of a cloudy marine boundary layer capped by an inversion is considered. Only the initial CCN concentration is varied so as to yield clouds with varying degrees of collection. Domain average calculations of τ and S are performed to evaluate the effect that the collection has on cloud optical properties.

The rest of this paper is divided as follows. Section 2 examines the theory and rederives some important expressions for spectra undergoing collection. Section 3 presents results from box model simulations of collection as well as eddy-resolving model simulations.

2. Theory

The equation for τ in the visible region of the spectrum is given by

$$\tau \approx \int_{z_b}^{z_t}\int_0^{\infty} 2\pi r^2 n(r)\, dr\, dz, \tag{1}$$

where $n(r)$ defines the drop spectrum with respect to radius r, z_b is cloud base, and z_t is cloud top, and the extinction efficiency has been assumed to be equal to 2. For a homogeneous cloud, (1) reduces to

$$\tau \approx 2\pi N^{1/3}\left[\frac{3\mathrm{LWC}}{4\pi\rho_w}\right]^{2/3} f(\sigma)h, \tag{2}$$

where ρ_w is the density of water, $h = z_t - z_b$ is the cloud depth, and $f(\sigma)$ is some function of the breadth of the spectrum. At constant LWC, constant h, and constant spectral breadth,

$$\tau = CN^{1/3}, \tag{3}$$

and C is a constant [e.g., *Platnick and Twomey*, 1994]. A simple expression relating cloud albedo A to optical depth is given by [*Bohren*, 1980]

$$A \approx \frac{(1-g)\tau}{2 + (1-g)\tau}, \tag{4}$$

which, although only approximate, is sufficient for our purposes. Cloud susceptibility S_0, defined [*Twomey*, 1991] as

$$S_0 = \left.\frac{dA}{dN}\right|_{\text{const LWC},h,\sigma} = \frac{\partial A}{\partial \tau}\frac{d\tau}{dN}, \tag{5}$$

can be reduced (using (3) and (4)) to

$$S_0 = \frac{A(1-A)}{3N}. \tag{6}$$

Pincus and Baker [1994] suggested, on the basis of a mixed-layer model formulation, that cloud depth is regulated by N through the production of drizzle, and relaxed the assumption of constant h. They showed that on the basis of their parameterized model formulation,

$$S = S_0\left[1 + \frac{5N}{h}\frac{dh}{dN}\right] = S_0[1 + \delta], \tag{7}$$

implying that S_0 is a lower bound estimate of S. The value of δ was shown to vary between about 0.5 at high N and 2 at very low N, although these values are largely dependent on the parameterizations in their model. Thus the enhancement in S due to variations in cloud depth associated with drop number is expected to be a maximum at low N.

At this point a few words on the concept of susceptibility are in order. As defined by (5), S represents the albedo response of a cloud to a change in drop concentration N. This concept, introduced by *Twomey* [1991], has been interpreted as the change in albedo due to a change in N for steady state boundary layers [e.g., *Pincus and Baker*, 1994], although the latter requirement need not be a necessary one. For S to be a useful concept, $A(N)$ must be well behaved (i.e., be a continuous, single-valued function with continuous first derivatives). It may well be that $A(N)$, defined in the sense of Pincus and Baker, is neither continuous nor single valued; for example, *Baker* [1990] suggests that boundary layers have two stable states in specific CCN regimes and that stable states are not achievable in intermediate regimes. In such cases, A is not defined for all N. Alternatively, one could consider a more general definition of susceptibility, one in which N refers to the local (in time and space) concentration of cloud drops with no equilibrium constraints. Such a situation corresponds better to actual clouds (which are not in steady state balance with their forcings) and avoids the issue of existence. However, this definition does retain the uniqueness problem, in that one could imagine that different transients could give different values of A and its first derivative. Problems of uniqueness and existence may very well undermine the utility of the concept of susceptibility, but for the present, and in the absence of evidence to the contrary, we assume that $A(N)$ is well behaved. In this case values of S derived from a temporally evolving cloud will be the same as those derived from steady state calculations.

As was discussed in the introduction, (1)–(7) may not be applicable to spectra undergoing broadening. According to (2), a dependence of τ on $N^{1/3}$ is expected only for $f(\sigma)$ = constant, and yet it is known that collection results in an increase in spectral breadth. Let us assume that the drop spectrum is described by the lognormal size distribution

$$n(r) = \frac{N}{(2\pi)^{1/2}\ln\sigma r}\exp\left[-\ln^2(r/r_g)/(2\ln^2\sigma)\right]. \tag{8}$$

It is then easy to show that $f(\sigma) = e^{\ln^2\sigma}$. Although the creation of a second mode means that one lognormal function does not reproduce the second drizzle mode, typical drop spectra measured in stratocumulus [*Nicholls*, 1984; *Boers et al.*, 1996] show that the drizzle mode is far less pronounced than the cloud droplet mode, so that fitting one lognormal function to observed spectra for illustrative purposes is reasonable. Using (8) and (2) yields

$$\frac{\tau}{\tau_0} = \left(\frac{N}{N_0}\right)^{1/3} \frac{e^{\ln^2\sigma_0}}{e^{\ln^2\sigma}} \tag{9}$$

with the subscript 0 implying a value at time 0 before the onset of collection. Because $\sigma > \sigma_0$, one obtains

$$\frac{\tau}{\tau_0} \leq \left(\frac{N}{N_0}\right)^{1/3}, \tag{10}$$

implying that the scaling of τ with $N^{1/3}$ is an upper limit of the expected response.

When considering susceptibility, the expression (5) for S is rederived, but the requirement that σ be constant is relaxed. In these simple calculations, cloud depth h and LWC are constant,

$$d\tau = \frac{\partial\tau}{\partial N} dN + \frac{\partial\tau}{\partial\sigma} d\sigma, \tag{11}$$

and using (2) with $f(\sigma) = e^{-\ln^2\sigma}$, and (3),

$$d\tau = \frac{\tau}{3N} dN - 2\tau \frac{\ln\sigma}{\sigma} d\sigma \tag{12}$$

or

$$\frac{d\tau}{\tau} = \frac{1}{3}\frac{dN}{N} - 2\ln\sigma\frac{d\sigma}{\sigma}. \tag{13}$$

Assuming for simplicity that during a time step the relative increase in σ due to collection is a factor χ times the relative decrease in N, or $d\sigma/\sigma = -\chi(dN/N)$, then,

$$\frac{d\tau}{\tau} = (\tfrac{1}{3} + 2\chi\ln\sigma)\frac{dN}{N}. \tag{14}$$

If one substitutes a typical value of $\sigma = 1.4$ or $\ln\sigma = 0.34$ [*Nakajima and King*, 1990] and assumes $\chi = 1$, one arrives at the result

$$\frac{d\tau}{dN} \approx \frac{\tau}{N} \tag{15}$$

and not the result derived from (3)

$$\frac{d\tau}{dN} = \frac{\tau}{3N}. \tag{16}$$

More generally, and without any assumptions about σ and χ, (14) yields the inequality

$$\frac{d\tau}{dN} > \frac{\tau}{3N}, \tag{17}$$

implying that the classical result for drop spectra of constant breadth is a minimum estimate of susceptibility.

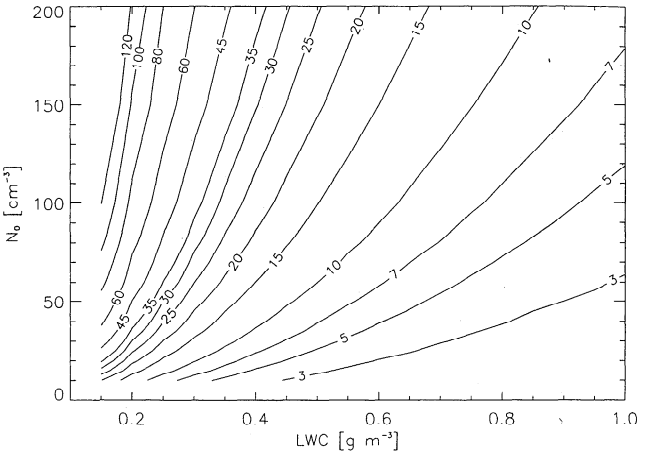

Figure 1. Box model results of the time (in minutes) required for 10% depletion in τ for drop spectra initially defined by (N_0, LWC), evolving through collection.

3. Results and Discussion

3.1. Box Model Calculations of Collection

Since drop collection conserves mass and thus meets the requirement of constant LWC used in the equations in section 1, the effect of drop collection on N and τ is examined in a simple, zero-dimensional box model of stochastic collection [*Tzivion et al.*, 1987]. The solution is based on a multimoment approach that conserves LWC by design. Comparison of the numerical solution with analytical solutions for simple kernels shows excellent agreement with no anomalous spreading. Further details are given by *Tzivion et al.* [1987]. The initial conditions for this model are N_0, LWC, and an assumed drop dispersion. Initial spectra are assumed to be lognormal with a geometric standard deviation σ of 1.4 (relative dispersion of 0.35). The LWC is varied over the interval (0.15 g m^{-3}–1.1 g m^{-3}), and N_0 is varied over the range (10 cm^{-3}–500 cm^{-3}).

Optical depth. The model is integrated with time, and at each time, τ and N are calculated and compared with the initial values. Figure 1 shows the results of these simulations in (LWC, N_0) space as contours of the time required for τ to be depleted by 10%. It is noted that for a given N_0, the time required for 10% depletion in τ decreases with increasing LWC. For a given LWC the time required for 10% depletion in τ increases with increasing N_0. This can be explained by the dependence of collection on the number concentration of drops larger than about 20 μm, above which size drop collection efficiencies become significant.

Next the stochastic collection model is run for 10 min, a typical parcel in-cloud residence time for a stratocumulus-capped boundary layer [*Stevens et al.*, 1996], over the same parameter space as in Figure 1. Figure 2 displays the depletion in τ as a function of the depletion in number to the one-third power. One sees that the depletion in τ simply due to spectral broadening is consistently larger than the corresponding depletion in $N^{1/3}$ predicted by (3). This clearly demonstrates the importance of spectral broadening on τ. The degree to which τ is depleted beyond that predicted by the depletion in $N^{1/3}$ depends on the amount of spectral broadening; these results show that depletion is a relative maximum when $(N/N_0)^{1/3} = 0.4$ and occurs for an N_0 of 50 cm^{-3} and LWC of 1.1 g m^{-3}; it is a relative minimum for negligible depletion (low LWC and large N). This result is important because it indicates that for

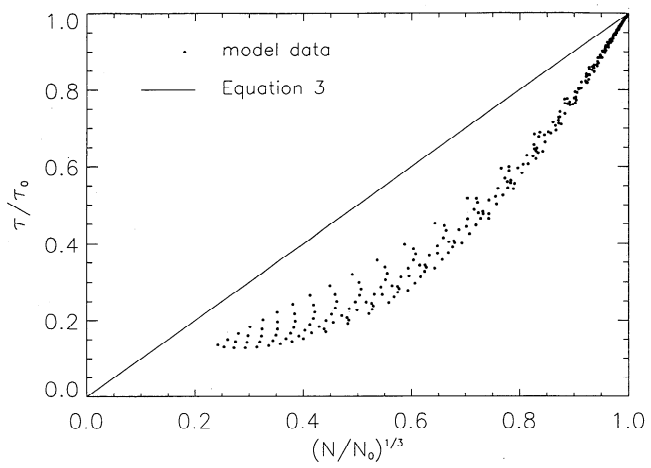

Figure 2. Depletion in τ as a function of the cubed-root depletion in number after 10 min of collection. Box model results are indicated by dots; the straight line is predicted by equation (3).

a fixed cloud depth and LWC, the change in albedo (which is proportional to the change in τ) due to drizzle formation is at a maximum for specific values of LWC and N and not necessarily for the largest LWC, smallest N pair. The largest LWC, smallest N pair does achieve the maximum broadening and greatest reduction in N, but when N is this low (and thus mean drop size is already large), τ is commensurately low, and further reduction due to depletion in N and broadening is not optimal. The results do depend on the initial value of σ, the time available for collection, and the collection kernel used, but all have a consistent, qualitative picture.

Susceptibility. A box model solution to collection for specified initial conditions (LWC = 0.5 g m^{-3}, N_0 = 50 cm^{-3}, σ_0 = 1.4) is run, and S is calculated as $\Delta A/\Delta N$ for a 2-s time step. Figure 3 shows that S increases faster than would be predicted by (6) but slower than the curve predicted by the rough assumptions yielding (15). A curve fit to these results suggests that

$$\frac{d\tau}{dN} \approx \frac{\tau}{1.2N}, \tag{18a}$$

which is in agreement with (17). It should be borne in mind that this is an empirical result based on a numerical solution to the collection equation, for a specific kernel, and for one set of initial conditions. The kernel used here is an approximate form suggested by *Long* [1974]. Use of a kernel compiled by *Hall* [1980] yields a slower rate of growth and

$$\frac{d\tau}{dN} \approx \frac{\tau}{1.6N}. \tag{18b}$$

Although this analysis does not provide an analytical formula for $d\tau/dN$, it is valuable because it again shows that S_0 as given by (6) is a minimum value of susceptibility.

Following (7), we may write

$$S_0[1 + \delta] = \frac{A(1-A)}{3N}[1 + \delta] = \frac{A(1-A)}{\alpha N} \tag{19}$$

where from (18), α = 1.2, or α = 1.6. This yields δ = 1.5 for (18a), or δ = 0.9 for (18b). In other words, the enhancement in S due to broadening lies between 0.9 and 1.5 for the calculations in Figure 3. These values are of the same order of magnitude as those calculated by *Pincus and Baker* [1994] for enhancement due to cloud depth response. The enhancement in S is entirely a consequence of the spectral broadening; although changes in N necessarily imply changes in S, these changes would not be over and above those predicted by classical theory (equation (6)).

3.2. Eddy-Resolving Model Results

The eddy-resolving model (ERM) is a two-dimensional (2-D) version of the large eddy simulation model described in detail by *Stevens et al.* [1996] and *Feingold et al.* [1996a]. The strength of this model lies in its emphasis on both dynamics and microphysics through the coupling of an explicit, warm, microphysical model [*Tzivion et al.*, 1987; *Stevens et al.*, 1996] with a dynamical model that resolves the large eddies. Thus cloud and drizzle formation respond to resolved eddy motions: CCN are activated to drops (depending on supersaturation, which is in turn related to updraft w); drop growth through condensation (evaporation) and stochastic collection is explicitly calculated; drizzle in-cloud residence is related to size-dependent fall velocity and local w. Although the 2-D ERM does not represent the eddy structure correctly compared with its three-dimensional (3-D) large eddy simulation counterpart, it does include the essential interactions between large eddies and cloud microphysical properties and provides a valuable framework for testing hypotheses without enormous computational expense.

A number of experiments have been performed using the ERM. The runs are initiated from the *Betts and Boers* [1990] July 7 stratocumulus sounding [see *Feingold et al.*, 1996b]. A constant CCN concentration of either 25 cm^{-3} (at a supersaturation of 1%), 50 cm^{-3}, 100 cm^{-3}, or 250 cm^{-3} is used throughout the domain. Only longwave radiation (responding to LWC) is simulated. The 50 cm^{-3} case exhibits significant drop number depletion (on the order of 60% over 3 hours (Figure 4)) but with negligible wet deposition (<0.1 mm d^{-1} at the surface); LWP achieves a quasi-steady state after about 110

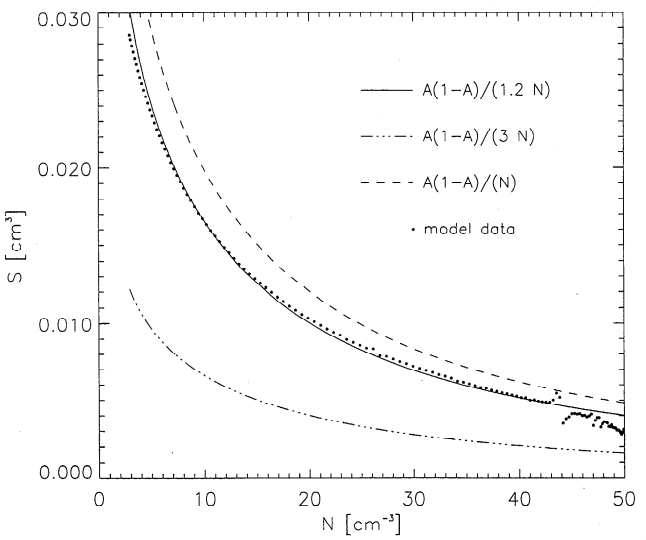

Figure 3. Increase in S resulting from depletion in N associated with collection in a box model calculation. The box model output is indicated by dots. The various line types indicate theoretical or empirical relations as described in the text.

min (Figure 4), assisting in interpretation of the results within the framework of constant LWP. For the CCN = 25 cm^{-3} case, drizzle does deplete LWC and LWP, but all intercomparisons between model runs are performed for constant LWP.

The output from the ERM is used in this analysis in the following manner: The cloud average values of τ, N, A, and h are calculated over a domain size roughly 3 km in the horizontal. The cloud covers the entire domain in all cases. In this regard, the calculations simulate an average measurement that might be obtained by satellite remote sensors. No attempt is made here to examine the smaller-scale effects associated with cloud inhomogeneities on the model grid (50 m in the horizontal by 25 m in the vertical). Although these effects are expected to be important, they are not the subject of this paper.

Figure 5 shows just one representation of the data, namely a τ-LWP plot after *Stephens* [1978]. Each point represents the average state of the cloud layer beginning at time 1 hour and calculated at 5-min intervals. (The first hour of simulation is regarded as a spin-up time during which the boundary layer eddies are developing from an initially quiescent state and is thus not included in the analysis.) Because $r_e \approx 1.5\text{LWP}/\tau$, the slope of this plot is inversely proportional to the drop effective radius r_e, as indicated by the dotted lines. It is noted that the runs with CCN = 250 cm^{-3} and CCN = 100 cm^{-3} are represented by points that form straight-line plots that are indicative of a constant r_e. Because drop collection is minimal in these two runs, attention is now focused on the CCN = 50 cm^{-3} and CCN = 25 cm^{-3} runs.

The plot for CCN = 50 cm^{-3} shows points initially evolving in time from positions at lower (LWP, τ) in the direction of higher (LWP, τ). As collection proceeds and N is depleted, points evolve toward larger r_e and smaller τ, but at quasi-steady LWP (Figure 4). For example, r_e increases 1.5-fold from about 14 μm (at 110 min) to 20 μm (at 180 min) at approximately constant LWP; under the latter constraint, $(\tau_2/\tau_1) \simeq (r_{e1}/r_{e2})$, indicating a decrease in τ of 30%. With albedo close to linear in τ in this region (equation (4)), a similar reduction in albedo is implied. These are large numbers and strongly indicate the importance of the collection process in reducing cloud albedo, even without wet removal.

The run with CCN = 25 cm^{-3} in Figure 5 shows a temporal evolution with r_e initially at 16 μm, but soon followed by increasingly larger r_e. A maximum LWP of just over 105 g m^{-2} is reached, after which the points move in a clockwise fashion toward lower τ, higher r_e, and lower LWP as wet deposition depletes cloud water.

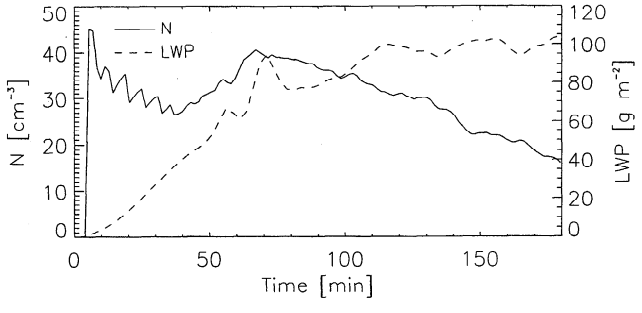

Figure 4. Temporal evolution of cloud-averaged fields from the eddy-resolving model: LWP and N for the run with 50 cm^{-3} CCN.

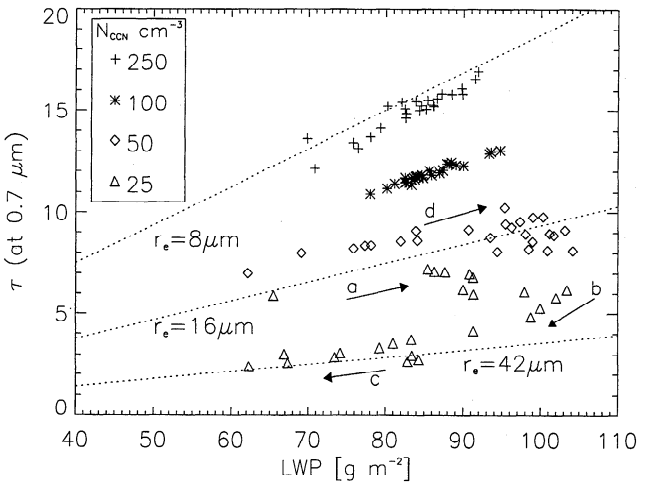

Figure 5. LWP-τ representation of ERM results for four initial CCN concentrations (25 cm^{-3}, 50 cm^{-3}, 100 cm^{-3}, and 250 cm^{-3}). The dotted straight lines represent the relationship $\tau = 1.5\ \text{LWP}/r_e$. Arrows labeled a, b, and c indicate the approximate direction of temporal evolution for the 25 cm^{-3} case. The arrow labeled d indicates the direction of temporal evolution for the 50 cm^{-3} case.

Optical depth. Figure 6 displays the data from the 2-D model in the same manner as was used in Figure 2 for the box model collection calculations. All data are displayed for clouds at different stages of their evolution, the only requirement being that they are of equivalent LWP (within 2.5%). Thus clouds displaying not only different N, but also different spectral form (resolved into 25 size bins), are compared. For example, a point with $\tau/\tau_0 \ll 1$ and $(N/N_0)^{1/3} \ll 1$ represents a comparison between drop spectra that have very different size spectra: one with large N, small r_e, and narrow breadth, and the other with small N, larger r_e, and greater breadth.

Figure 6 shows that the ratio τ/τ_0 (where $\tau < \tau_0$) is consistently smaller than that of the ratio $(N/N_0)^{1/3}$. For larger $(N/N_0)^{1/3}$ (i.e., spectra with similar numbers of drops) the

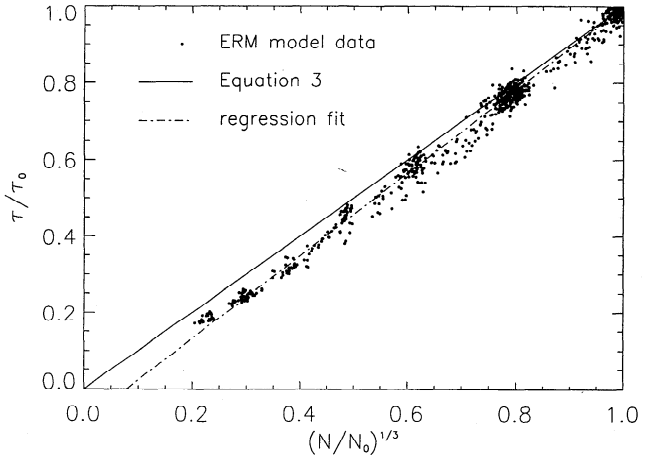

Figure 6. Depletion in τ as a function of the depletion in number to the one-third power. Each data point represents a comparison of two realizations of the eddy-resolving model where the requirement is that LWP is the same (within 2.5%). The solid straight line represents equation (3). Also shown is a linear regression to the data points (dash-dot line).

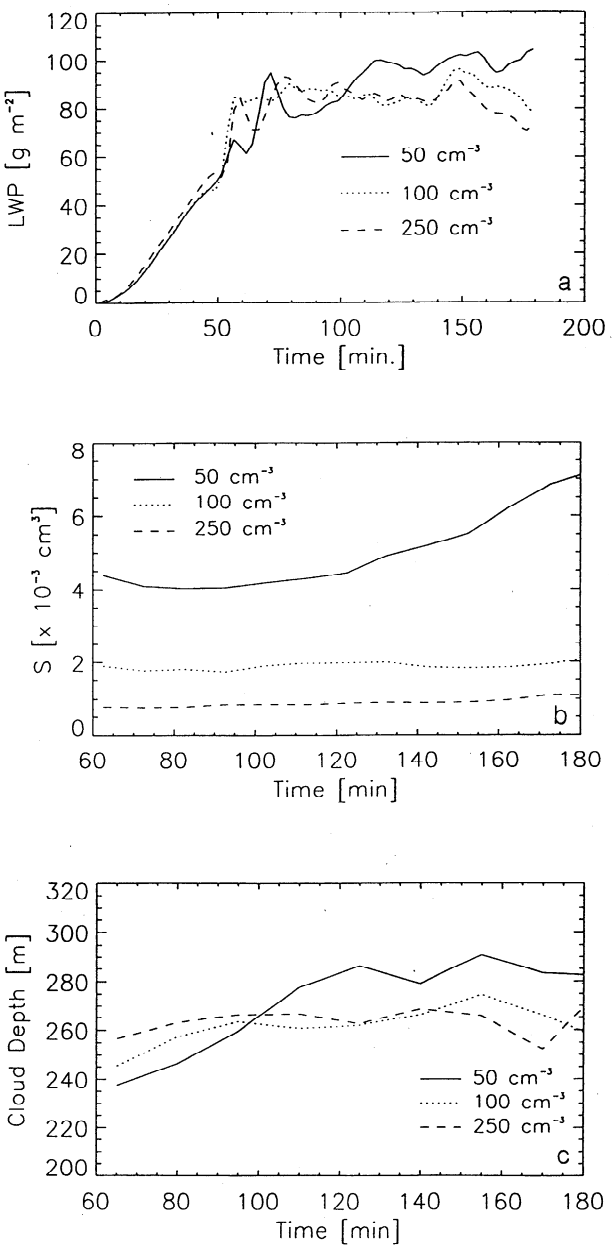

Figure 7. Change in (a) cloud LWP, (b) cloud susceptibility S, and (c) cloud depth as a function of time and initial CCN concentration for eddy-resolving model runs with 50 cm^{-3}, 100 cm^{-3}, and 250 cm^{-3}.

points tend to be closer to the 1:1 line and converge to the behavior predicted by (3). A linear regression fit to the data yields

$$\frac{\tau}{\tau_0} = 1.08\left(\frac{N}{N_0}\right)^{1/3} - 0.09. \qquad (20)$$

This empirical fit is shown primarily to exhibit the consistent offset of the optical depth response to N from the classical value predicted by (3) for small values of $(N/N_0)^{1/3}$, rather than as a reliable predictor of the system response to the collection process.

Susceptibility. Calculations of S are now performed for the three runs that do not exhibit a loss of cloud water through wet deposition. Only the post-spin-up period ($t > 60$ min) is of interest. It is noted that the intercomparison of these cases is strictly valid only at constant LWP, and because LWP tends to fluctuate, one has to be cautious in the interpretation of the results. Figure 7a shows that although LWP for the three runs is closely correlated, LWP for the 50 cm^{-3} case tends to be slightly larger (by about 6%, over the last 2 hours of simulation) than corresponding values for CCN = 100 cm^{-3} and 250 cm^{-3}. This may be a result of small amounts of drizzle in the 50 cm^{-3} case creating evaporative cooling just below the cloud base that destabilizes the subcloud layer and feeds back to stronger cloud motions, which in turn generate higher LWP. A similar conclusion was arrived at by *Feingold et al.* [1996a] and *Stevens* [1996] based on their model results for weakly drizzling clouds. Other, undetermined, sources of this difference may also exist.

Figure 7b shows calculations of S for the three runs. Equation (18b) has been used in the calculation of S; use of (18a) would result in higher estimates of S. The most appropriate expression for S is not critical for now, as it is the temporal change in S that is of interest. (See discussion of Figure 8 below.) Although the 100 and 250 CCN cm^{-3} runs exhibit minimal collection, inclusion of these data sets in the analysis provides a comparison between differences in S due to differences in CCN concentration, and hence differences in N (250 CCN cm^{-3} versus 100 CCN cm^{-3}), and differences in S due to collection (the 50 cm^{-3} run exhibiting drop number depletion and spectral broadening with time). One sees that S increases progressively with decreasing initial CCN concentration. For the runs with 250 cm^{-3} and 100 cm^{-3} there is no significant change in S; over the course of the run they differ by a factor of ≈2, a value closely tied to the difference in N. On the other hand, the run with 50 cm^{-3} CCN shows a fairly rapid increase in S (≈60%) as drop number N is depleted through collection (to a similar degree) without significant change in LWP (Figure 4). The actual values of S have implicit in them the effect of spectral broadening since the constant 1.6 (equation (18b)), rather than 3 (equation (16)), was used in their calculation, and because the calculation of A is derived from spectra that have been broadened by collection; the relative change in S, however, is purely a function of the depletion in N, and is the same regardless of whether (18b) or (16) is used. This is in accord with the analysis in section 3.1 that showed that decreases in N alone, would not enhance S over and above that predicted by (6).

Figure 7c shows that cloud depth remains fairly constant for each of the runs once they have reached a quasi-equilibrium and that their average values differ by only about 3%, suggesting that any enhancement in S due to changes in cloud depth as proposed by *Pincus and Baker* [1994] is expected to be small for this particular case. However, it is noteworthy that in the general case, enhancement in S due to spectral broadening is expected to work in unison with effects related to cloud depth; according to Pincus and Baker, as CCN concentration is reduced, the enhancement in S increases owing to the cloud depth response to N; simultaneously, there is an expected enhancement in S due to broadening associated with collection, that also increases with decreasing CCN concentration.

Finally, the ERM output for the CCN = 50 cm^{-3} run is used to examine the validity of (6). Figure 8a is a plot of A versus N, the slope of which determines S. The best fit to these points (calculated at 5-min intervals for $t > 110$ min) produces $S = 3.8 \times 10^{-3}$. If S is now calculated according to (6) (Figure 8b), the points lie below 3.8×10^{-3}, indicating that (6) is an

underestimate of S, in accord with (17) and the box model results for collection only. Thus spectral broadening has resulted in an enhancement in S.

In comparing Figures 7b and 8, it is apparent that the best fit value for S for this run (i.e., 3.8×10^{-3}) is somewhat lower than the values plotted in Figure 7b (derived from (18b)); the exact expression to be used in calculating S when drop spectra exhibit broadening is not well defined. Further examination of Figure 3 shows that at values of S of the order of 3×10^{-3}, the data points lie closer to the curve given by (6) than they do when S is, say, 5×10^{-3}. This analysis varies as a function of initial conditions used as input to the box model, and given that the ERM's cloud domain comprises spectra with many different combinations of LWC, N, and σ, placing more accurate bounds on (17) appears difficult. In general, however, these ERM results do support the claim that S calculated using (6) tends to be an underestimate of the true S.

4. Summary and Conclusions

This paper has examined the impact of drop collection on the optical properties of stratocumulus clouds using models of varying complexity. The intent has been to evaluate whether commonly used expressions relating parameters such as cloud optical depth τ, drop number N, albedo A and susceptibility S are generally applicable to spectra that undergo broadening as a result of collection.

Demonstrations using a box model of stochastic collection show that the changes in drop spectral form, caused by collection, are such that τ does not scale with $N^{1/3}$, as is the case for narrow cloud drop spectra with constant breadth. In addition, this model has been used to demonstrate that cloud susceptibility as calculated by (6) for drop spectra of constant breadth is a minimum and that when collection is active, S may be up to about 2.5 times larger than the conventional calculation. If the effect of spectral broadening on S is cast in the same framework as that of *Pincus and Baker* [1994], a calculation of the relative enhancement factor δ, yields $\delta = 1.5$. This factor was calculated for a relatively small range of N values ($N < 50$ cm^{-3}). When compared with the δ calculated by Pincus and Baker (due to cloud depth changes), over a similar range of concentrations, we find that δ due to spectral broadening is as large as that associated with cloud depth changes. This is an important result and indicates that collection is an important modifier of susceptibility. Moreover, since both effects are expected to increase with decreasing N, (6) is expected to be an even lower estimate of S than was previously suggested.

Simulations with an eddy-resolving model used to examine the change in cloud microphysical and optical properties as a function of initial CCN concentrations provide support for the result that τ does not scale with $N^{1/3}$ for clouds with an active collection process. In addition, it is shown that cloud susceptibility can increase quite dramatically (on the order of 60%) due to a similar order of magnitude depletion in drop concentration associated with collection. The eddy-resolving model results also indicate an enhancement in S resulting from spectral broadening, but it is not as strong as that seen in the box model. This suggests that in natural clouds, one might expect the increase in susceptibility to be derived primarily from the decrease in drop concentration resulting from collection, with spectral broadening of secondary importance, at least for the conditions simulated in this paper.

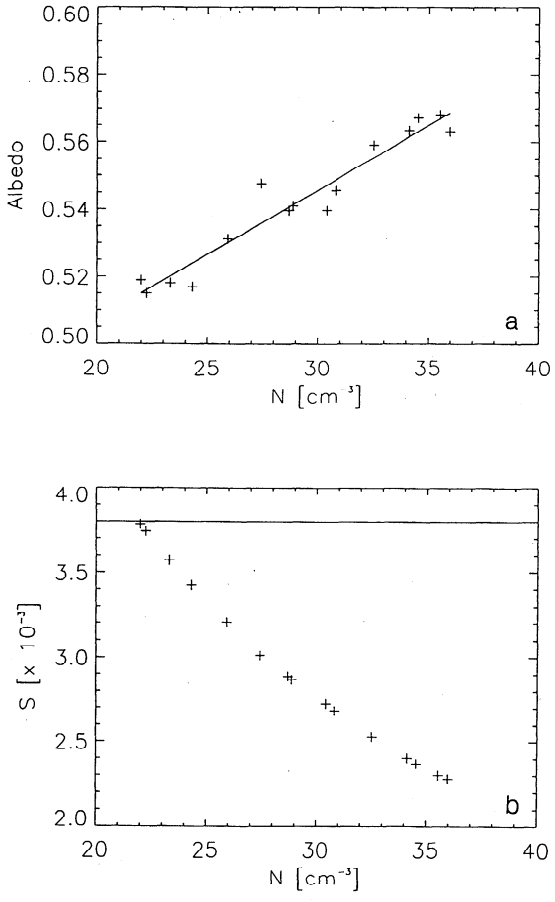

Figure 8. Analysis of the CCN = 50 cm^{-3} run for $t > 110$ min: (a) A versus N, and (b) cloud susceptibility S calculated using equation (6) versus N. The best fit to the points in Figure 8a indicates $S = 3.8 \times 10^{-3}$. This value is shown as the solid horizontal line in Figure 8b. Note that all points in Figure 8b lie below this line, indicating that (6) underestimates S.

Acknowledgments. This research was partially supported by grants from the Office of Naval Research (N00014-93-F0029) and the DOD/ISSO Lidar Wind Program. Additional support came from the Environmental Sciences Division of the U.S. Department of Energy under contract DE-FG03-95ER61958 as part of the Atmospheric Radiation Measurement Program. One of the authors (G.F.) thanks the CSIRO Division of Atmospheric Research for hosting him while some of this research was completed.

References

Albrecht, B., Effects of precipitation on the thermodynamic structure of the trade wind boundary layer, *J. Geophys. Res.*, *98*, 7327–7337, 1993.

Albrecht, B. A., D. A. Randall, and S. Nicholls, Observations of marine stratocumulus clouds during FIRE, *Bull. Am. Meteorol. Soc.*, *69*, 618–626, 1988.

Albrecht, B. A., C. S. Bretherton, D. Johnson, W. H. Schubert, and A. S. Frisch, The Atlantic Stratocumulus Transition Experiment—ASTEX, *Bull. Am. Meteorol. Soc.*, *76*, 889–904, 1995.

Austin, P. H., Y. Wang, R. Pincus, and V. Kujala, Precipitation in stratocumulus clouds: Observational and modelling results, *J. Atmos. Sci.*, *52*, 2329–2352, 1995.

Baker, M., Bistability of CCN concentrations and thermodynamics in the cloud topped boundary layer, *Nature*, *345*, 142–145, 1990.

Betts, A. K., and R. Boers, A cloudiness transition in a marine boundary layer, *J. Atmos. Sci.*, *47*, 1480–1497, 1990.

Boers, B., J. B. Jensen, P. B. Krummel, and H. Gerber, Microphysical and shortwave radiative structure of wintertime stratocumulus

clouds over the Southern Ocean, *Q. J. R. Meteorol. Soc.*, *122*, 1307–1339, 1996.

Bohren, C. F., Multiple scattering of light and some of its observable consequences, *Am. J. Phys.*, *55*, 524–533, 1980.

Bretherton, C. S., P. Austin, and S. T. Siems, Cloudiness and marine boundary layer dynamics in the ASTEX Lagrangian experiments, II, Cloudiness, drizzle, surface fluxes, and entrainment, *J. Atmos. Sci.*, *52*, 2724–2735, 1995.

Feingold, G., B. Stevens, W. R. Cotton, and A. S. Frisch, On the relationship between drop in-cloud residence time and drizzle production in stratocumulus clouds, *J. Atmos. Sci.*, *53*, 1108–1122, 1996a.

Feingold, G., S. M. Kreidenweis, B. Stevens, and W. R. Cotton, Numerical simulation of stratocumulus processing of cloud condensation nuclei through collision-coalescence, *J. Geophys. Res.*, *101*, 21,391–21,402, 1996b.

Frisch, A. S., C. W. Fairall, and J. B. Snider, On the measurement of stratus cloud and drizzle parameters with a K_α-band Doppler radar and a microwave radiometer, *J. Atmos. Sci.*, *52*, 2788–2799, 1995.

Hall, W. D., A detailed microphysical model within a two-dimensional dynamical framework: Model description and preliminary results, *J. Atmos. Sci.*, *37*, 2486–2507, 1980.

Kogan, Y. L., M. P. Khairoutdinov, D. K. Lilly, Z. N. Kogan, and Q. Liu, Modelling of stratocumulus cloud layers in a large eddy simulation model with explicit microphysics, *J. Atmos. Sci.*, *52*, 2923–2940, 1995.

Leaitch, W. R., G. A. Issac, J. W. Strapp, C. N. Banic, and H. A. Wiebe, The relationship between cloud droplet number concentrations and anthropogenic pollution: Observations and climatic implications, *J. Geophys. Res.*, *97*, 2463–2474, 1992.

Long, A. B., Solutions to the droplet collection equation for polynomial kernels, *J. Atmos. Sci.*, *31*, 1040–1052, 1974.

Moeng, C.-H., Large eddy simulation of a stratus-topped boundary layer, I, Structure and budgets, *J. Atmos. Sci.*, *43*, 2886–2900, 1986.

Nakajima, T., and M. D. King, Determination of the optical thickness and effective particle radius of clouds from reflected solar radiation measurements, I, Theory, *J. Atmos. Sci.*, *47*, 1878–1893, 1990.

Nicholls, S., The dynamics of stratocumulus, *Q. J. R. Meteorol. Soc.*, *110*, 821–845, 1984.

Pincus, R., and M. B. Baker, Effect of precipitation on the albedo susceptibility of clouds in the marine boundary layer, *Nature*, *372*, 250–252, 1994.

Platnick, S., and S. Twomey, Determining the susceptibility of cloud albedo to changes in droplet concentration with the advanced very high resolution radiometer, *J. Appl. Meteorol.*, *33*, 334–347, 1994.

Slingo, A., A GCM parameterization for the shortwave radiative properties of water clouds, *J. Atmos. Sci.*, *46*, 1419–1427, 1989.

Stephens, G. L., Radiation profiles in extended water clouds, I, Theory, *J. Atmos. Sci.*, *35*, 2111–2122, 1978.

Stevens, B., On the dynamics of precipitating stratocumulus, Pap. 618, 140 pp., Colo. State Univ., Fort Collins, 1996.

Stevens, B., G. Feingold, R. L. Walko, and W. R. Cotton, On elements of the microphysical structure of numerically simulated nonprecipitating stratocumulus, *J. Atmos. Sci.*, *53*, 980–1006, 1996.

Twomey, S., The nuclei of natural cloud formation, II, The supersaturation in natural clouds and the variation of cloud droplet concentration, *Geofis. Pura Appl.*, *43*, 243–249, 1959.

Twomey, S., Pollution and the planetary albedo, *Atmos. Environ.*, *8*, 1251–1256, 1974.

Twomey, S., The influence of pollution on the short wave albedo of clouds, *J. Atmos. Sci.*, *34*, 1149–1152, 1977.

Twomey, S., Aerosols, clouds and radiation, *Atmos. Environ., Part A*, *25*, 2435–2442, 1991.

Tzivion, S., G. Feingold, and Z. Levin, An efficient numerical solution to the stochastic collection equation, *J. Atmos. Sci.*, *44*, 3139–3149, 1987.

Warren, S. G., C. J. Hahn, J. London, R. M. Chervine, and R. L. Jenne, Global distribution of total cloud cover and cloud type amounts over ocean, *Tech. Note NCAR/TN-317+STR*, 42 pp., Natl. Cent. for Atmos. Res., Boulder, Colo., 1986.

R. Boers, Division of Atmospheric Research, CSIRO, Aspendale, Victoria 3195, Australia.

W. R. Cotton and B. Stevens, Department of Atmospheric Science, Colorado State University, Fort Collins, CO 80523.

G. Feingold, Environmental Technology Laboratory, NOAA, 325 Broadway, Boulder, CO 80303. (e-mail: gfeingold@etl.noaa.gov)

(Received November 20, 1996; revised March 20, 1997; accepted March 26, 1997.)